

**REPORT DOCUMENTATION PAGE**

Form Approved OMB No. 0704-0188

Public reporting burden for this collection of information is estimated to average 1 hour per response, including the time for reviewing instructions, searching existing data sources, gathering and maintaining the data needed, and completing and reviewing the collection of information. Send comments regarding this burden estimate or any other aspect of this collection of information, including suggestions for reducing the burden, to Department of Defense, Washington Headquarters Services, Directorate for Information Operations and Reports (0704-0188), 1215 Jefferson Davis Highway, Suite 1204, Arlington, VA 22202-4302. Respondents should be aware that notwithstanding any other provision of law, no person shall be subject to any penalty for failing to comply with a collection of information if it does not display a currently valid OMB control number.  
**PLEASE DO NOT RETURN YOUR FORM TO THE ABOVE ADDRESS.**

<b>1. REPORT DATE (DD-MM-YYYY)</b> 11-05-2006	<b>2. REPORT TYPE</b> Final Report	<b>3. DATES COVERED (From – To)</b> 15 August 2005 - 15-May-06
--	---------------------------------------	---

<b>4. TITLE AND SUBTITLE</b>  Development Of Electro-Spark Alloying (ESA) And Thermo-Reactive Electro-Spark Surface Strengthening (TRESS) Technologies And Set Of Equipment With Attachments For Mechanization	<b>5a. CONTRACT NUMBER</b> FA8655-03-D-0001, Delivery Order 0024
	<b>5b. GRANT NUMBER</b>
	<b>5c. PROGRAM ELEMENT NUMBER</b>

<b>6. AUTHOR(S)</b>  Professor Evgeny A Levashov	<b>5d. PROJECT NUMBER</b>
	<b>5d. TASK NUMBER</b>
	<b>5e. WORK UNIT NUMBER</b>

<b>7. PERFORMING ORGANIZATION NAME(S) AND ADDRESS(ES)</b> Moscow State Institute of Steel and Alloys (Technological University) Leninsky Prospect, 4 Moscow 119049 Russia	<b>8. PERFORMING ORGANIZATION REPORT NUMBER</b>  N/A
---	--

<b>9. SPONSORING/MONITORING AGENCY NAME(S) AND ADDRESS(ES)</b>  EOARD PSC 802 BOX 14 FPO 09499-0014	<b>10. SPONSOR/MONITOR'S ACRONYM(S)</b>
	<b>11. SPONSOR/MONITOR'S REPORT NUMBER(S)</b> EOARD Task 05-9004

**12. DISTRIBUTION/AVAILABILITY STATEMENT**  
Approved for public release; distribution is unlimited.

**13. SUPPLEMENTARY NOTES**

**14. ABSTRACT**

This report results from a contract tasking Moscow State Institute of Steel and Alloys (Technological University) as follows: The main goal of the project is to develop advanced ESA and TRESS coating technologies for application on Ti and superalloys substrates to resist high-cycle fatigue failure initiated at the blade roots. The bar and disc electrodes will be manufactured by self-propagating high temperature synthesis (SHS) method. Mechanical activation for systems with low exothermal effect will be applied. The influence of the SHS process parameters (combustion rate and temperature, stoichiometry of the initial reaction mixture, dispersivity of the reagent powders, etc.) on the structure and phase composition of the composite electrodes and the influence of the SHS-densification parameters (densification pressure, time under pressure, delay time of densification after initiation of the combustion reaction) on the porosity and physical-mechanical properties of the electrodes will be investigated. Hard, wear-, corrosion- and oxidation resistant coatings (up to 300 μm thick) based on oxides, carbides, silicates, borides and nitrides of transition metals will be studied. Coating hardness, friction and wear behavior, corrosion, and oxidation resistance will be investigated. Fabrication and transfer to AFRL/MLBT of a set of ESA equipment with attachments for mechanization and a number of various disk and bar electrodes made of composite materials based on carbides, borides, nitrides, intermetallics strengthened by nanoparticles.

**15. SUBJECT TERMS**  
EOARD, Electro Spark Alloying, Surface Strengthening, Thermo Reactive Electro Spark Strengthening

<b>16. SECURITY CLASSIFICATION OF:</b>			<b>17. LIMITATION OF ABSTRACT</b> UL	<b>18. NUMBER OF PAGES</b>  17	<b>19a. NAME OF RESPONSIBLE PERSON</b> JOAN FULLER
<b>a. REPORT</b> UNCLAS	<b>b. ABSTRACT</b> UNCLAS	<b>c. THIS PAGE</b> UNCLAS			<b>19b. TELEPHONE NUMBER (Include area code)</b> +44 (0)20 7514 3154

## GRANT ASSISTANCE PROGRAM

### PROJECT AGREEMENT # RUE-1506-MO-05

PROJECT TITLE: Development of Electro-spark Alloying (ESA) and Thermo-Reactive Electro-spark Surface Strengthening (TRESS) Technologies and Set of Equipment with Attachments for Mechanization

PROJECT DIRECTOR: Evgeny Levashov

Principal Organization: Moscow State Institute of Steel and Alloys (Technological University)

Address: Leninsky pr. 4, 164  
Moscow 119049  
Russian Federation

Reporting number: Final report

The report consists of:

Summary

Introduction

1. Experimental

2. Electrode materials

3. XRD of ES coatings and their structure

3.1. ES coatings deposited with TiC–NiAl–ZrO<sub>2</sub><sup>nano</sup> electrodes

3.2. TiC–Cr<sub>3</sub>C<sub>2</sub>–Ni–ZrO<sub>2</sub><sup>nano</sup>-based coatings

3.3. TiB<sub>2</sub>–TiAl–NbC<sup>nano</sup>-based coatings

4. Coatings Microhardness, Thickness and Continuity

5. Tribological behavior of coatings: Friction coefficient and wear resistance

Concluding remarks

6. The electrodes

7. The equipment for deposition of electrospark coatings

Future work

## **Summary**

Electro-spark alloying (ESA) is attracting much attention in preparing protective coatings. ESA provides some obvious advantages in comparison with other deposition methods such as high adhesion, low cost, relatively high productivity, relative simplicity and compactness of equipment, ecological safety. The advantage of local coating deposition, minimal substrate heating, and high coating thickness (up to 1 mm) are especially beneficial for anti-fretting wear protective coatings, which may be applied to Ti and superalloy blade roots in turbine engines to resist wear and fatigue. The main goal of the project is to develop advanced Electro-Spark Alloying (ESA) and Thermo-Reactive Electro-Spark Surface Strengthening (TRESS) coating technologies for application on Ti and superalloys substrates to resist high-cycle fatigue failure initiated at the blade roots. Provide AFRL with advanced bar and disc TiC-,TiB-based electrodes for ESA manufactured by Self-propagating High-temperature Synthesis (SHS) method. Provide AFRL with ESA deposition equipment with attachments for mechanization at the end of the project.

## Introduction

Further advance in industrial implementation of electrospark alloying (ESA) is closely related to the quality of coatings deposited by this technique. In its turn, the quality of coatings depends (a) on the composition of anode (electrode material) and cathode (substrate) and (b) on deposition conditions.

For these studies, we selected the following new electrode materials: TiC–NiAl (Ti–C–Ni–Al system), TiC–Ni alloy (Ti–C–Ni alloy system), TiB<sub>2</sub>–TiAl (Ti–B–Al system), and TiC–Cr<sub>3</sub>C<sub>2</sub>–Ni (Ti–C–Cr–Ni system). All materials produced using forced SHS-pressing were doped with nano-sized additives (NbC, ZrO<sub>2</sub>, WC–Co, W, WC, and Al<sub>2</sub>O<sub>3</sub>).

After preliminary testing, the following advanced electrode materials TiC–NiAl–ZrO<sub>2</sub><sup>nano</sup>, TiC–Cr<sub>3</sub>C<sub>2</sub>–Ni–ZrO<sub>2</sub><sup>nano</sup> and TiB–TiAl–NbC<sup>nano</sup> were selected.

## 1. Experimental

Electrospark (ES) coatings were deposited with a universal apparatus Alier-Metal 2002. We could vary the frequency and energy of current pulses, their duration/amplitude, and the frequency of vibroexciter (normally 600 Hz).

The titanium alloy was used as a substrate.

The kinetics of mass transfer (cathode weight increment, erosion of anode material) was measured gravimetrically. Deposition conditions were optimized for each individual electrode material.

Elemental composition was determined with an electron microscope JSM-6700F equipped with a JED-2300F (JEOL) accessory for energy dispersive spectrometry (EDS). An image was formed at an accelerating voltage of 15 kV.

Metallographic analysis was carried with an optical microscope Neophot-32 and/or Axiovert 25 CA (Zeiss).

Microhardness ( $H\mu$ ) was measured with a PMT-3 instrument at a 100-g load.

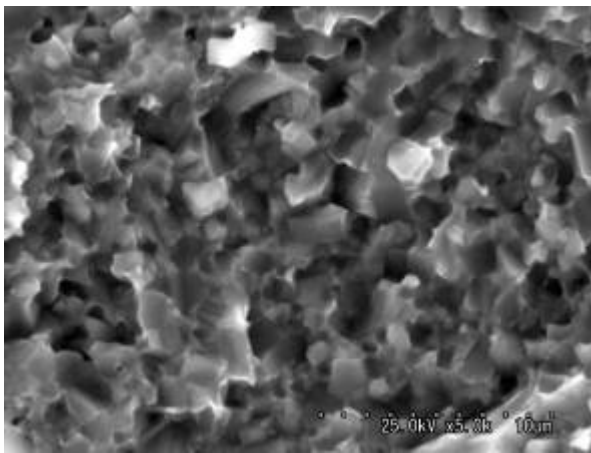
The friction coefficient ( $\mu$ ) was measured with a tribometer (CSM Instruments) operating in the ball-on-disc mode. The balls of WC–Co (3 mm in diameter) were used as

a static partner. Coated samples were rotated at a linear velocity of 10 cm/s under a load of 5 N. The data obtained were continuously computer-processed (software InstrumX). Before testing, the surface of coating was slightly polished.

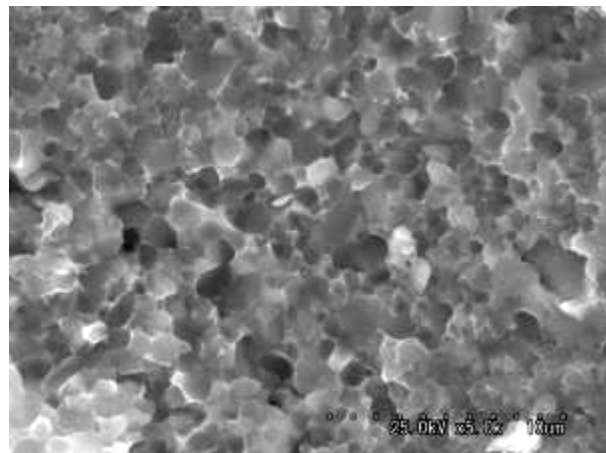
## 2. Electrode materials

We explored the effect of SHS parameters (applied pressure, time under load, time lag between the initiation of SHS and loading) on the structure, porosity, and mechanical properties of resultant electrode materials. Doping with nano-sized refractory component (added to a green mixture) was found to modify the structure of electrode materials.

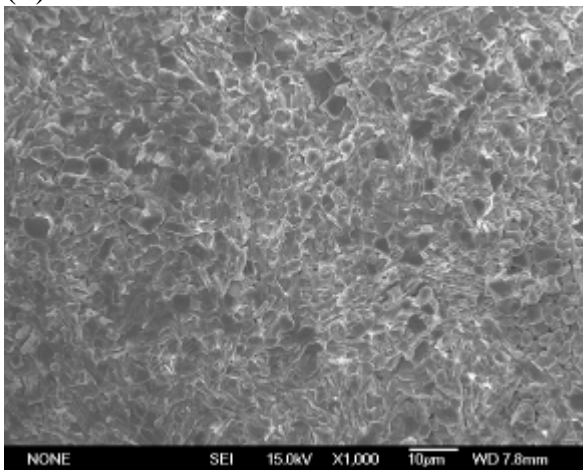
Typical structure (fractures) of the electrode materials adopted for ES deposition is given in Figs. 1 *a,b,c*.



(a)



(b)



(c)

(a)  $\text{TiC-NiAl-ZrO}_2^{\text{nano}}$

(b)  $\text{TiC-Cr}_3\text{C}_2\text{-Ni-ZrO}_2^{\text{nano}}$

(c)  $\text{TiB-TiAl-NbC}^{\text{nano}}$

Fig. 1. Typical microstructure of electrode materials (fractures).

### 3. XRD of ES coatings and their structure

#### 3.1. ES coatings deposited with TiC–NiAl–ZrO<sub>2</sub><sup>nano</sup> electrodes

The conditions for deposition of ES coatings with TiC–NiAl–ZrO<sub>2</sub><sup>nano</sup> electrodes (are given in Table 1.

Table 1. Deposition conditions

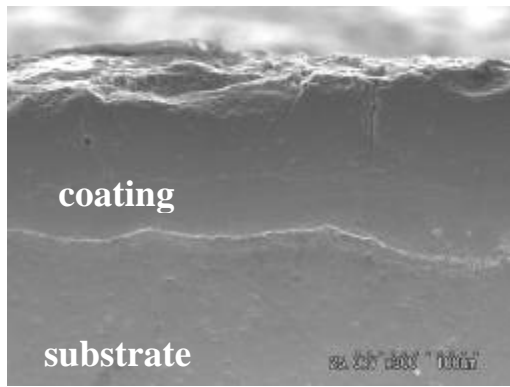
Discharge current $I$ , A	Current pulse duration $\tau$ , $\mu$ s	Repetition frequency $f$ , Hz	Pulse energy $E$ , J	Deposition time $t$ , min/cm <sup>2</sup>
170	25	1300	0.13	10

The XRD data for these coatings are presented in Table 2. The Ti (C,N) phase is seen to be predominant (69 vol %).

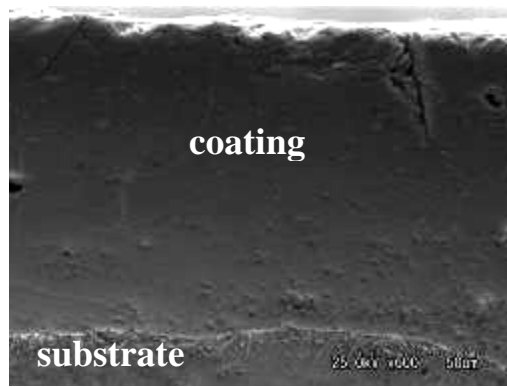
Table 2. Data of XRD analysis of coating

Phase	Str. type	Vol. fraction, %	Lattice parameters, Å
alpha-Ti ( type A3 )	hP2/1	4.2 ± 0.1	A= 2.949 C= 4.736
Ti (C,N) ( type B1 )	cF8/2	69 ± 0.1	A= 4.273
Ti-X ( beta, type A2 )	cI2/1	1.6 ± 0.0	A= 3.256
Ni <sub>2</sub> Ti Al ( type L2.1 )	cF16/3	25.2 ± 0.1	A= 5.906

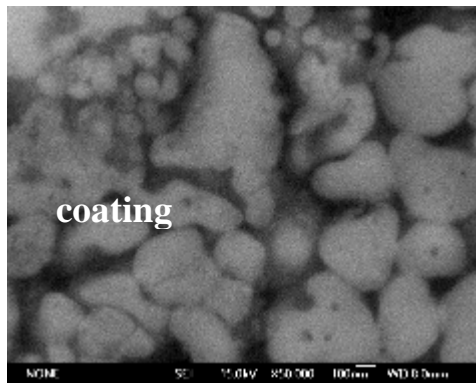
The structure of the coating is shown in Figs. *a–c*. The absence of cracks at the coating–substrate boundary evidences for a high adhesion of coating to substrate. During deposition, a substrate material is known to undergo partial mixing with an electrode material. As follows from Fig. 2*c* a deposited coating is formed by fine particulates below 300 nm in size. Note that the size of TC grains in the electrode material attains a value of 1–3  $\mu$ m. Therefore, the structure of coating is more fine-grained compared to that of starting electrode material: this can be associated with recrystallization via the liquid phase formed in the channel of pulsed discharge.



(a)  $\times 300$



(b)  $\times 600$



(c)  $\times 50000$

Fig.2 Structure of TiC–NiAl– ZrO<sub>2</sub><sup>nano</sup> -based coating.

The kinetics of mass transfer (substrate weight increment, erosion of electrode material) is given in Fig.3

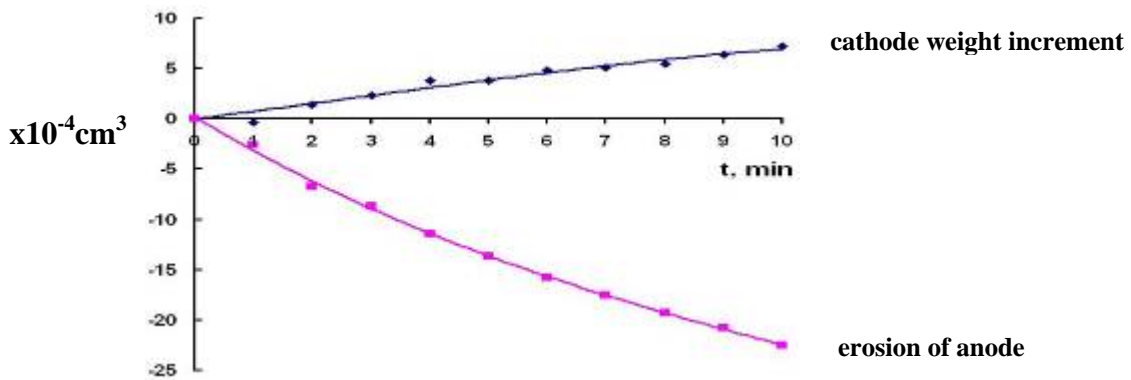


Fig.3

### 3.2. TiC–Cr<sub>3</sub>C<sub>2</sub>–Ni–ZrO<sub>2</sub><sup>nano</sup> -based coatings

Deposition conditions are characterized in Table 3.

Table 3. Deposition conditions

Discharge current $I$ , A	Current pulse duration $\tau$ , $\mu$ s	Repetition frequency $f$ , Hz	Pulse energy $E$ , J	Deposition time, min/cm <sup>2</sup>
170	25	500	0.13	10

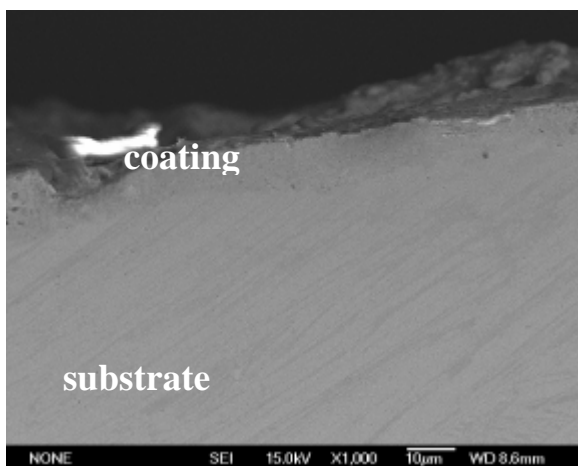
As follows from Table 4, the TiC phase is predominant (80 vol %). The high-temperature  $\gamma$ -Fe phase is fixed upon quenching.

The microstructure of TiC–Cr<sub>3</sub>C<sub>2</sub>–Ni–ZrO<sub>2</sub><sup>nano</sup> -based coating is presented in Figs. 3a, b. Again, no cracks between the coating and substrate were found. The coating is formed by particulates below 150–200 nm in size. Note that the size of carbide grains in the electrode material was about 1–2  $\mu$ m.

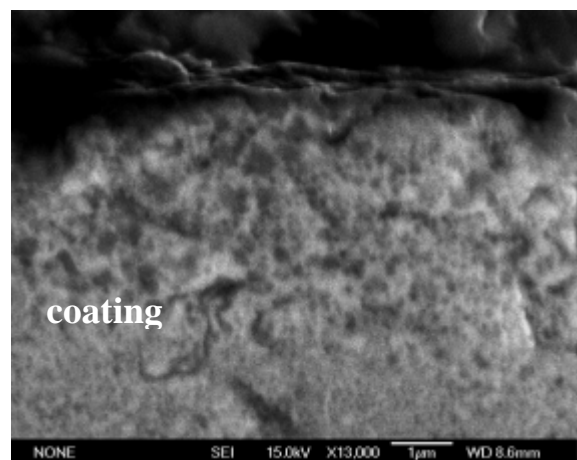
Table 4. \*Data of XRD analysis of coating

Phase	Str. type	Vol. fraction, %	Lattice parameters, Å
Ti C (type B1)	cF8/2	80	$A = 4.320$
$\gamma$ -Fe (type A1)	cF4/1	13	$A = 3.634$
$\alpha$ -Fe (type A2)	cI2/1	7	$A = 2.883$

\* steel substrate



(a)  $\times 1000$



(b)  $\times 13000$

Fig. 3. Structure of TiC–Cr<sub>3</sub>C<sub>2</sub>–Ni–ZrO<sub>2</sub><sup>nano</sup> -based coating

The kinetics of mass transfer (substrate weight increment, erosion of electrode material) is given in Fig.4.

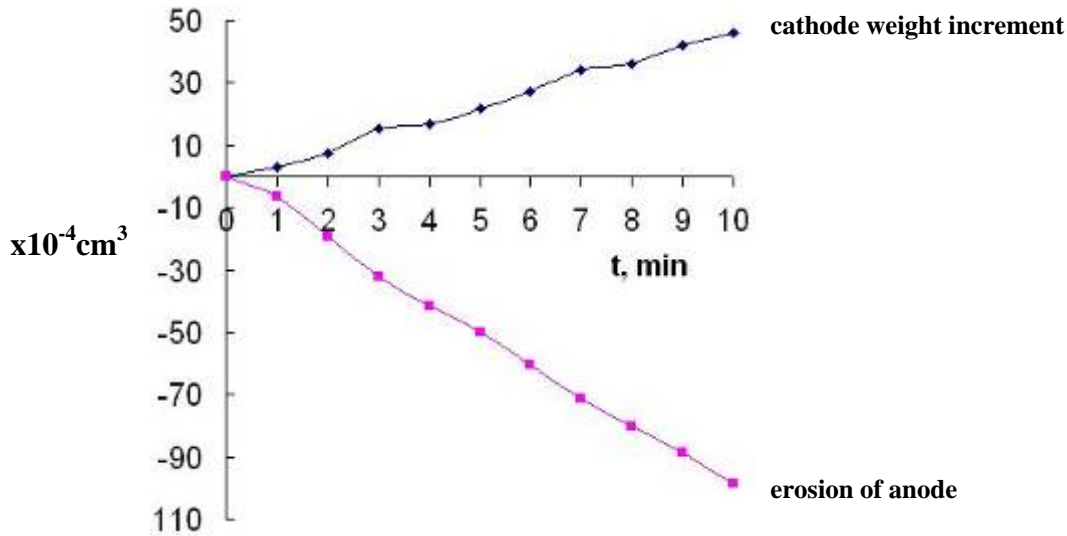


Fig.4.

### 3.3. TiB<sub>2</sub>-TiAl-NbC<sup>nano</sup>-based coatings

Deposition conditions are given in Table 5.

Table 5. Deposition conditions

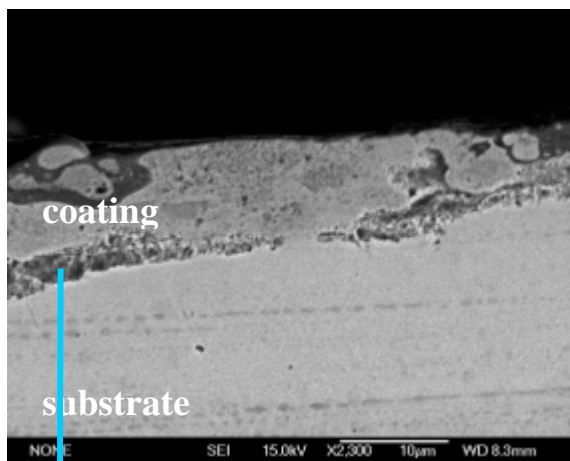
Discharge current $I$ , A	Current pulse duration $\tau$ , $\mu$ s	Repetition frequency $f$ , Hz	Pulse energy $E$ , J	Deposition time $t$ , min/cm <sup>2</sup>
170	25	1300	0.13	10

As follows from Table 6, the coating contains predominant the phases of TiB<sub>2</sub> (59,3 vol %) and TiB (30,2 vol %) .

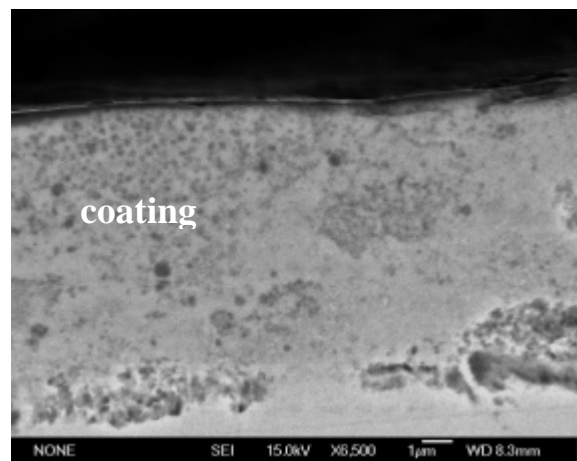
The microstructure of the coating deposited using TiB-TiAl-NbC<sup>nano</sup> electrode is presented in Figs. 5a-c. In contrast to TiC-NiAl-ZrO<sub>2</sub><sup>nano</sup>-based and TiC-Cr<sub>3</sub>C<sub>2</sub>-Ni-ZrO<sub>2</sub><sup>nano</sup> -based coatings, this coating are formed by larger particulates (1-4  $\mu$ m in size). Again, there are no cracks at the substrate-coating boundary.

Table 6. Data of XRD analysis of coating

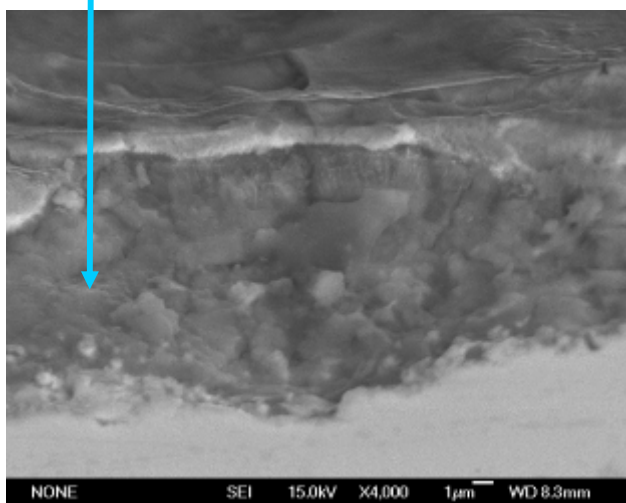
Phase	Str. type	Vol. fraction, %	Lattice parameters, Å
Ti B <sub>2</sub> ( type C32 )	hP3/4	59.3 ± 0.4	A= 3.026 C= 3.231
Ti B ( type B1 )	cF8/2	30.2 ± 0.4	A= 4.248
Ti N ( type B1 )	cF8/2	4.2 ± 0.2	A= 4.169
Ti(1-x) N(x) ( type A3 )	hP4/16	3.4 ± 0.2	A= 2.972 C= 4.773
Ti <sub>2</sub> Al N	hP8/4	2.9 ± 0.2	A= 2.958 C=13.764



(a) ×2300



(b) ×6500



(c) ×4000

Fig. 5. Microstructure of coatings deposited using TiB–TiAl–NbC<sup>nano</sup> electrode.

The kinetics of mass transfer (substrate weight increment, erosion of electrode material) is given in Fig.6

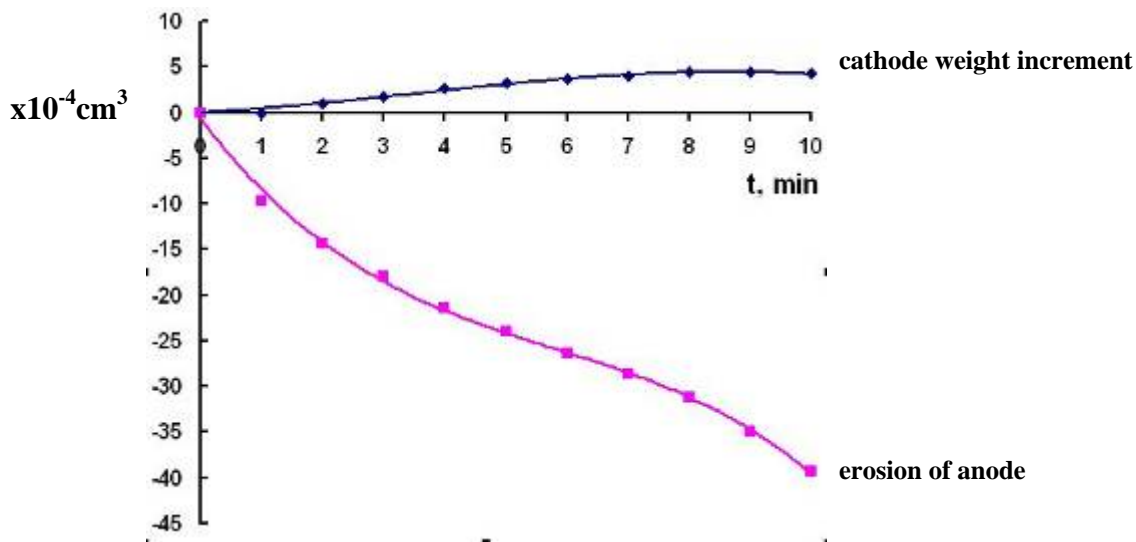


Fig.6

#### 4. Coatings Microhardness, Thickness and Continuity

The parameters of ES coatings formed on a Ti substrate are collected in Table 7. Coatings deposited in optimized conditions are seen to have a thickness of 40–50  $\mu\text{m}$  and continuity of 90–100%. The microhardness of coatings was found to vary within the range 13.2–14.2 GPa.

Table 7. Parameters of coatings (substrates: Ti-alloy)

Electrode material	Microhardness of coating, GPa	Thickness, $\mu\text{m}$	Continuity, %
TiC–NiAl–ZrO <sub>2</sub> <sup>nano</sup>	14.2	50	100
TiC–Cr <sub>3</sub> C <sub>2</sub> –Ni– ZrO <sub>2</sub> <sup>nano</sup>	13.8	60	90
TiB <sub>2</sub> –TiAl–NbC <sup>nano</sup>	13.5	40	90

\*Microhardness of Ti- alloy is 2.0 GPa

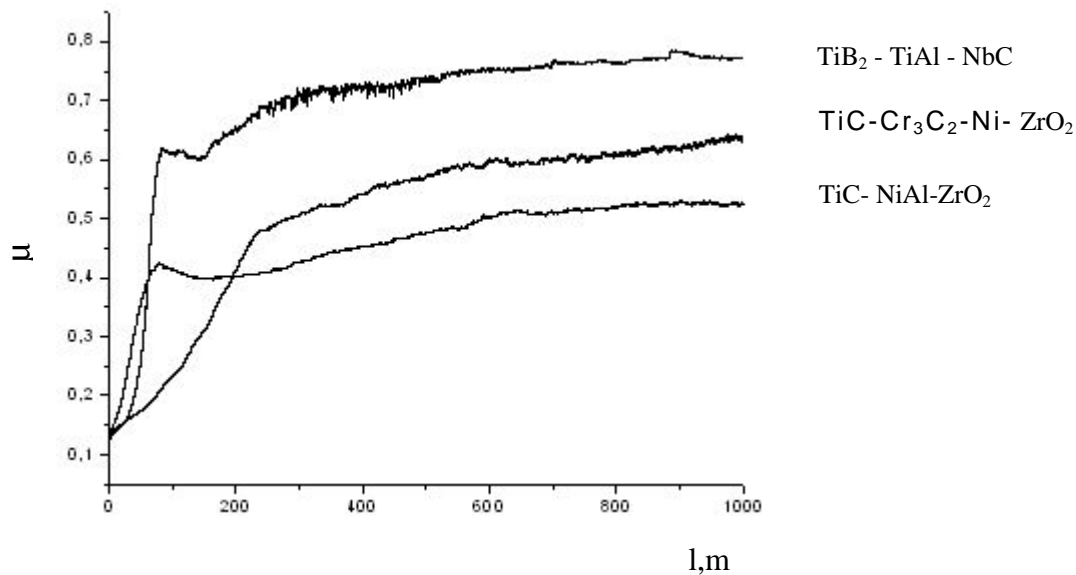
## 5. Tribological behavior of coatings: Friction coefficient and wear resistance

Tribological testing conditions are characterized in Table 8.

Table 8. Testing conditions

Static partner	Static partner material	Linear velocity, cm/s	Load, N	Run, m	Track radius, mm
Ball 3 mm in diameter	WC+6Co	10	5	1000	4.4

The data for friction coefficient  $\mu$  are presented in Fig. 7.



### 7. Friction coefficient for ES- coatings deposited using different electrode materials.

As is seen in Fig. 7, the  $\mu$  values are within the range 0.48–0.76. A least value was found for the pair 'counter body  $\text{TiC-NiAl-ZrO}_2^{\text{nano}}$  based coating' while a largest one, for the pair 'counter body  $\text{TiB}_2\text{-TiAl-NbC}^{\text{nano}}$  based coating'.

High  $\mu$  values for the coating in the case of electrode of  $\text{TiB-TiAl-NbC}$  can be explained by a coarse-grained structure of this coating. For carbide coatings with a fine-grained structure,  $\mu = 0.48$

For ES- coatings, it seems impossible to calculate the absolute value of wear resistance because the roughness of coating is greater than the depth of wear track. The typical overall view of wear tracks is shown in Figs. 8a–c.

In order to diminish  $\mu$ , it seems reasonable to fill the pores of coatings with a solid lubricant, such as molybdenum disulfide  $\text{MoS}_2$ . Due to high roughness of ES coatings, the solid lubricant can be retained on their surface, irrespective of operation conditions.

The  $\mu$  values as a function of static partner run for TiB–TiAl–NbC-based coating with (1) and without (2) solid lubricant are given in Fig. 9. In the presence of lubricant, the  $\mu$  values are seen to be lower by a factor of 2.5.

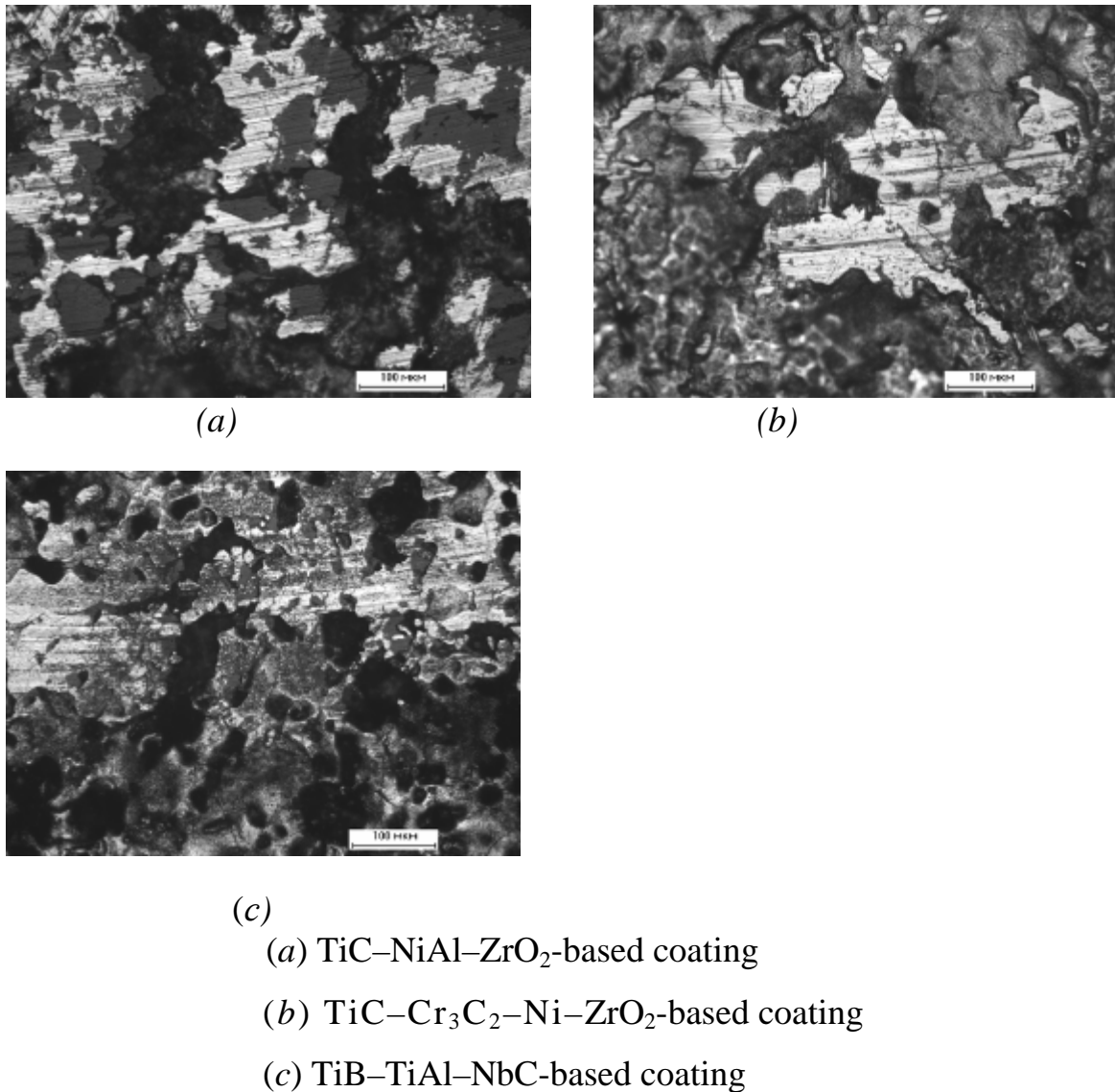


Fig. 8. Overall view of wear tracks on the surface of ES coating.

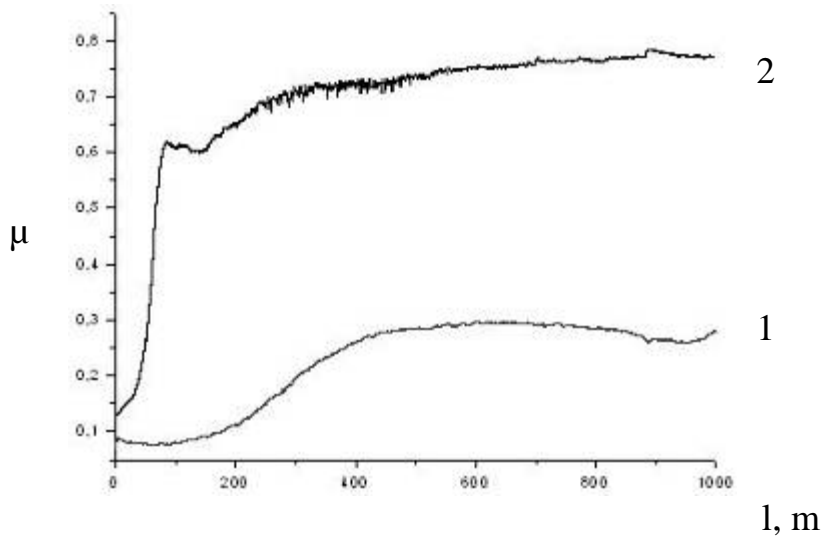


Fig. 9. Values  $\mu$  as a function of counter body run  $l$  for TiB-TiAl-NbC-based coating with (1) and without (2) lubricant.

The wear resistance can be estimated indirectly from the wear of static partner. The relevant data are presented in Fig. 10 and Table 9. The largest wear of static partner was caused by TiC-NiAl-ZrO<sub>2</sub>-based coating (Figs. 11a-c), which can be associated with the affinity of substrate to coating material. The lowest wear of counter body ( $0.29 \cdot 10^{-6} \text{ mm}^3 \text{ N}^{-1} \text{ m}^{-1}$ ) was observed in case of TiB-TiAl-NbC-based coating.

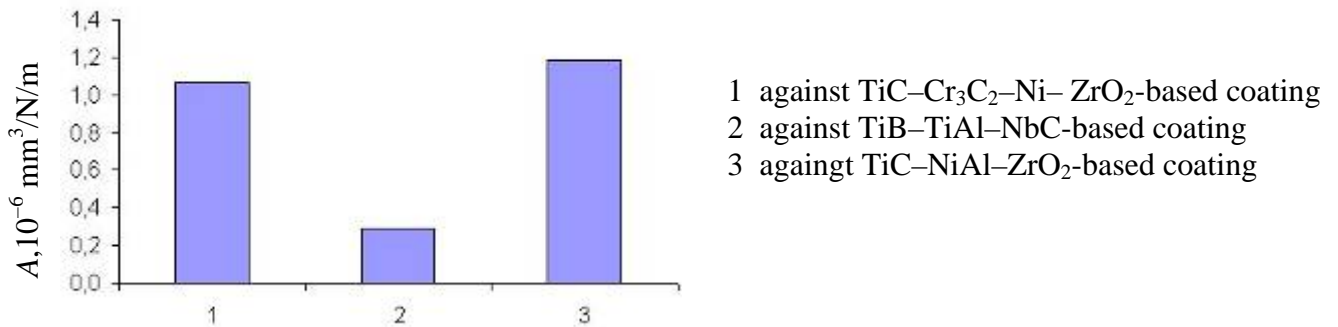
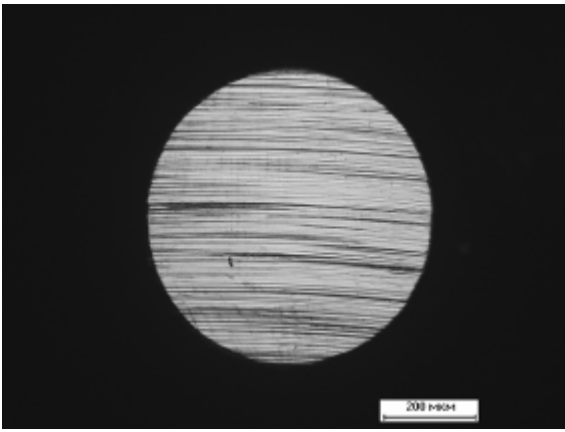


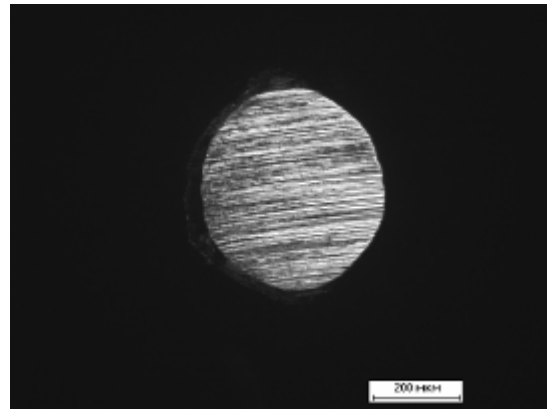
Fig.10. Wear of static partner caused by different coatings.

Table 9. Wear of static partner

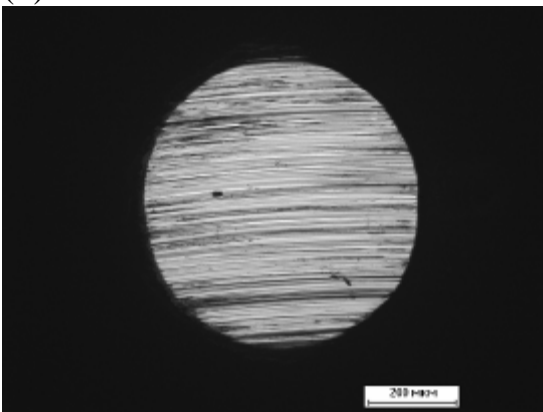
Electrode material	$A, 10^{-6} \text{ mm}^3/\text{N/m}$
TiC-Cr <sub>3</sub> C <sub>2</sub> -Ni- ZrO <sub>2</sub>	1.07
TiB-TiAl-NbC	0.29
TiC-NiAl-ZrO <sub>2</sub>	1.19



(a)



(b)



(c)

(a) TiC–Cr<sub>3</sub>C<sub>2</sub>–Ni–NbC-based coating

(b) TiB–TiAl–NbC-based coating

(c) TiC–NiAl–ZrO<sub>2</sub>-based coating

Fig. 11. Wear of counter body caused by different coatings.

### Concluding remarks

We investigated the structure, composition, and properties of ES- coatings deposited onto an Ti-alloy substrate using SHS-produced electrode materials. Coatings deposited with TiC-based electrodes were found to have a lower grains size compared to those deposited with titanium boride electrodes. The use of ESA provides a 6.6–7.1-fold increase in the hardness of surface layer in compare with the substrate hardness. The friction coefficient of ES- coatings can be diminished upon introduction of a solid lubricant into their pores.

## 6. The electrodes

The bar and disk electrode materials  $\text{TiC-NiAl-ZrO}_2^{\text{nano}}$ ,  $\text{TiC-Cr}_3\text{C}_2\text{-Ni-ZrO}_2^{\text{nano}}$  and  $\text{TiB-TiAl-NbC}^{\text{nano}}$  (Fig.12) were produced.



Fig.12

## 7. The equipment for depositon electrosark coatings

The set of equipment for technology of electrosark depositon of coatings were designed , fabricated and verified.(Fig.13-Fig.18)

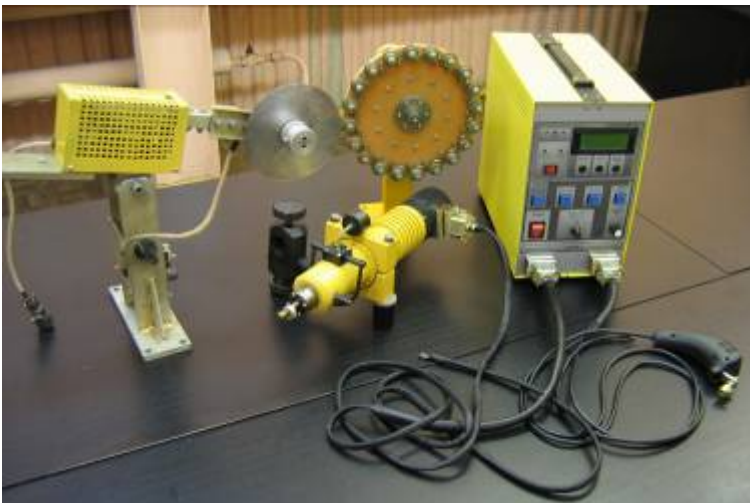


Fig.13 Complete set “Alier-Metal” for electrosark deposition of coatings



Fig.14 Power supply and control unit



Fig.15 Manual tool



Fig.16 Tool with rotating electrode for mechanization of deposition process of coating.



Fig.17 Multi-electrodes tool for mechanization of deposition process of coating.

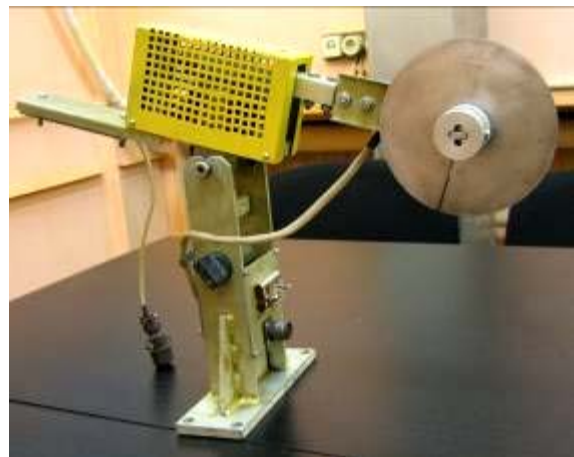


Fig.18 Tool with disk electrode for mechanization of deposition process of coating



Fig.18 Current brush

### **Future work**

Application of ESA and TRESS technologies for future in-house research projects at AFRL/MLBT for the deposition of hard, wear-, corrosion- and oxidation-resistant coatings up to 300  $\mu\text{m}$  thick for high temperature fretting wear prevention and fatigue control of turbine engines. Further advance/modify ESA and TRESS equipment for meeting needs in airspace application.